

TORSIONAL RIGIDITY, ISOSPECTRALITY AND QUANTUM GRAPHS

DON COLLADAY, LEON KAGANOVSKIY, AND PATRICK MCDONALD

ABSTRACT. We study torsional rigidity for graph and quantum graph analogs of well-known pairs of isospectral non-isometric planar domains. We prove that such isospectral pairs are distinguished by torsional rigidity.

1. INTRODUCTION

In 1966, Marc Kac offered a poetic formulation of what came to be a much studied problem involving the geometry of planar domains: Does Dirichlet spectrum determine a planar domain up to isometry? Kac’s problem inspired a great deal of work much of which centered on developments involving heat invariants. The appearance of Sunada’s work involving the construction of isospectral metrics for Riemannian manifolds provided powerful new methods for investigating diverse spectral phenomena; in particular, Sunada’s method led to the discovery of a number of negative results for inverse spectral problems. In 1992 Gordon, Web and Wolpert used an extension of Sunada’s method to construct a pair of isospectral, non-isometric planar domains [GWW]. Soon after, Buser, Conway Doyle and Semmler produced a collection of families of pairs of isospectral non-isometric planar polygonal domains (we refer to these examples as *BCDS pairs*). Their construction, again going back to Sunada, involves reflecting a “seed” triangle across edges (see [BCDS]). An example of their construction can be found in section 3 below and plays an important role in our work.

Given these negative results in reference to Kac’s question,¹ one might ask: What are good invariants for planar domains and/or quantum graphs?

One approach to finding new invariants is to use data which, while not spectral, arise from the normalized Dirichlet eigenfunctions in a natural fashion. An example is afforded by the sequence generated by counting nodal domains. This approach has been investigated in a recent series of papers in which quantum graph analogs of BCDS pairs are produced and their corresponding nodal domain counts are compared (see [BPB], [BSS]).

Another approach to producing non-spectral invariants is given by integration against the heat kernel. More precisely, suppose $p_D(t, x, y)$ is the Dirichlet heat kernel for the domain D and $u(t, x) = \int_D p_D(t, x, y) dy$ is the solution of the initial

1991 *Mathematics Subject Classification.* Primary 58J53.

Key words and phrases. quantum graphs, torsional rigidity, heat content, isospectrality.

¹For smoothly bounded domains Kac’s problem is still open.

value problem

$$\begin{aligned} \frac{\partial u}{\partial t} &= \Delta u \text{ on } (0, \infty) \times D \\ \lim_{t \rightarrow 0} u(t, x) &= 1. \end{aligned}$$

Then one can define the *heat content* of D

$$q_D(t) = \int_D u(t, x) dx$$

as well as a sequence of invariants

$$(1.1) \quad A_k = k \int_0^\infty t^{k-1} q_D(t) dt.$$

The invariant A_1 , sometimes referred to as the *torsional rigidity of the domain D* , can be computed via the solution of a Poisson problem. More precisely, if u_1 solves

$$\begin{aligned} \Delta u_1 &= -1 \text{ on } D \\ u_1 &= 0 \text{ on } \partial D \end{aligned}$$

then

$$A_1 = \int_D u_1(x) dx.$$

Torsional rigidity arises in the study of elasticity and has a long history (a source for early work is [Po1]). In addition to its role in the mechanics of solid bodies, torsional rigidity is closely related to the expected exit time of Brownian motion from the domain D and higher values of k in (1.1) correspond to higher moments of the exit time (cf [Mc1], [KMM] and references within). For this reason the sequence $\{A_k\}$ defined by (1.1) has been labeled the *L^1 -moment spectrum* associated to D .

It is easy to see that both heat content and the moment spectrum are invariants of the metric. Recent work suggest they play a valuable role in understanding fundamental geometric properties of a given ambient space (for example, isoperimetry [HMP1] [HMP2], [Mc2]), and one might reasonably ask how such objects compare to Dirichlet spectrum as tools to classify domain behavior up to isometry. Such a study has been initiated in [MM1]. For the purpose of this note, the main results of [MM1] can be summarized as follows:

- (1) For smoothly bounded domains, the moment spectrum determines the heat content.
- (2) For generic smoothly bounded domains, the moment spectrum determines the Dirichlet spectrum.

It is a result of Gilkey that heat content cannot distinguish isospectral planar domains constructed via the Sunada method [Gi1]. On the other hand, in [BDK], the authors establish that heat content distinguishes the isospectral domains constructed by Chapman and in [MM2] the authors construct combinatorial analogs of BCDS pairs and explicit check that their heat contents differ (at the fifth coefficient). The main result of this paper is that with respect to heat content, quantum graph analogs of BCDS pairs behave more like combinatorial graphs than planar domains, and that torsional rigidity is sufficient to distinguish well-known examples of isospectral pairs. More precisely, we have

Theorem 1.1. *Let D_1 and D_2 be the 7_1 -pair of isospectral non-isometric planar polygonal domains as constructed by Buser, Conway, Doyle and Semmler and let G_1 and G_2 be their quantum graph analogs (cf section 3 below). Then G_1 and G_2 are isospectral, non-isometric and distinguished by their torsional rigidity.*

In addition to establishing Theorem 1, we prove

Theorem 1.2. *The moment spectrum of a quantum graph with Dirichlet standard boundary conditions (cf section 2 below) determines the heat content of the quantum graph.*

As an immediate corollary, we conclude that our isospectral non-isometric pairs are distinguished by their heat content. Our technique applies to the other families of isospectral pairs constructed in [BCDS].

The remainder of this note is organized as follows. In the second section we establish the required background information concerning quantum graphs, establish our notational conventions and prove Theorem 1.2. In the third section we review the Sunada construction in the context of planar domains following Buser, Conway, Doyle and Semmler and include the construction of isospectral non-isometric quantum graph analogs of BCDS pairs. In the fourth section of the paper we explicitly compute the torsional rigidity for a pair of isospectral non-isometric quantum graphs and check they differ. We end the paper with a previously studied example ([MM2]) of a pair of isospectral non-isomorphic weighted combinatorial graphs which arise as analogs of BCDS pairs and check that they too are distinguished by their torsional rigidity.

2. QUANTUM GRAPHS

Let G be a graph with finite vertex set V and edge set E . For $v \in V$, denote by $d(v)$ the cardinality of the set $E_v = \{e \in E : v \in e\}$. We will often find it convenient to assign an orientation to edges; that is, for each edge $e = \{u, v\}$, choose $\mathcal{O}(e)$ to be either u or v .

By a *path* in G we will mean a sequence of vertices, $v_{i_1}, v_{i_2}, \dots, v_{i_m}$, with $\{v_{i_j}, v_{i_{j+1}}\} \in E$. We say G is connected if every pair of vertices can be connected by a path in G . We restrict our attention to graphs which are connected and contain no edges of the form $\{v, v\}$.

We endow G with a metric structure as follows. For each edge $e \in E$, choose a positive real number l_e . Identify each edge $e \in E$ with the interval $[0, l_e]$, where 0 is identified with $\mathcal{O}(e)$ and l_e is identified with the remaining vertex of e . This identification allows us to introduce a natural coordinate on each edge; the coordinate x_e along the interval $[0, l_e]$. These coordinates give rise to a natural metric structure for G . The pair $(G, \{l_e\}_{e \in E})$ is called a *metric graph*. Because G and l_e are finite, the resulting metric graph is compact.

We identify functions on $(G, \{l_e\}_{e \in E})$ with functions along the open edges together with values at each vertex: For $\phi : G \rightarrow \mathbb{C}$, we write $\phi = \oplus_{e \in E} \phi_e$. The metric structure on each edge gives rise to a natural Hilbert space associated to $(G, \{l_e\}_{e \in E})$. Write

$$\mathcal{H}_e = L^2([0, l_e])$$

where the inner product associated to edge e is defined by

$$\langle f, g \rangle_e = \int_0^{l_e} f(x_e) \overline{g(x_e)} dx_e.$$

Let

$$\mathcal{H} = \oplus_{e \in E} \mathcal{H}_e$$

and denote the inner product on \mathcal{H} by

$$\begin{aligned} \langle f, g \rangle &= \int_G f(x) \overline{g(x)} dx \\ &\equiv \sum_{e \in E} \langle f, g \rangle_e. \end{aligned}$$

In particular,

$$\langle 1, 1 \rangle = L(G)$$

where $L(G)$ is the total length of the graph G .

There is a natural differential operator acting on functions on the interior of each edge: $\frac{d^2}{dx_e^2}$. We wish to extend this operator to a self-adjoint operator on L^2 -functions on the metric graph. We sketch the approach developed in [KPS1] (see [KPS1] for details).

For each $e \in E$, let \mathcal{D}_e denote

$$\mathcal{D}_e = \{\phi_e \in \mathcal{H}_e : \phi_e, \phi_e' \text{ are absolutely continuous, } \phi_e'' \in \mathcal{H}_e\}.$$

Let

$$\mathcal{D}_e^0 = \{\phi_e \in \mathcal{D}_e : \phi_e(0) = \phi_e(l_e) = \phi_e'(0) = \phi_e'(l_e) = 0\}$$

and set

$$\begin{aligned} \mathcal{D} &= \oplus_{e \in E} \mathcal{D}_e \\ \mathcal{D}^0 &= \oplus_{e \in E} \mathcal{D}_e^0. \end{aligned}$$

Then the operator Δ^0 which acts on $\phi \in \mathcal{D}^0$ according to

$$(\Delta^0 \phi)_e(x) = \frac{d^2 \phi_e}{dx_e^2}(x_e)$$

is closed, symmetric and densely defined. We seek to impose boundary conditions which give self-adjoint extensions of Δ^0 to \mathcal{H} .

We begin by noting that boundary values of functions along edges lie in the space $\mathcal{B} = \mathbb{C}^{|E|} \times \mathbb{C}^{|E|}$ where the order of the components is fixed by the orientation. More precisely, given $\phi \in \mathcal{D}$, let $\underline{\phi} \in \mathcal{B}$ be given by

$$\underline{\phi} = (\{\phi_e(0)\}_{e \in E}, \{\phi_e(l_e)\}_{e \in E}).$$

Boundary conditions can then be described by a pair of linear operators $A, B : \mathcal{B} \rightarrow \mathcal{B}$ satisfying

$$A\underline{\phi} + B\underline{\phi}' = 0.$$

Those pairs of linear operators (A, B) leading to self-adjoint extensions of Δ^0 have been classified by Kostykin, Potthoff and Schrader [KPS1] using a symplectic formalism going back to at least to Novikov. We are interested in a single special case, *Dirichlet standard boundary conditions*, which we now describe.

Definition 2.1. Denote by DSBC the collection of continuous functions defined by

$$(2.1) \quad \text{DSBC} = \left\{ \phi \in \mathcal{D} : \begin{array}{ll} \phi(v) = 0 & \text{if } d(v) = 1 \\ \sum_{e \in E_v} \frac{d\phi}{d\nu_e}(v) = 0 & \text{if } d(v) \neq 1. \end{array} \right\}$$

where the derivative occurring in (2.1) is always directed into the vertex v and, as before, $E_v = \{e \in E : v \in e\}$ is the collection of edges on which v is incident.

We note that the literature often refers to "standard boundary conditions" as those involving Kirchhoff conditions at internal vertices (ie vertices of degree at least 2) and Neumann conditions at boundary vertices (ie vertices of degree 1).

We can describe standard boundary conditions using pairs of matrices (A, B) as follows: For each vertex v with $d(v) > 1$, introduce $d(v) \times d(v)$ matrices A and B (cf also [KPS1], [BPB])

$$A(v) = \begin{pmatrix} 1 & -1 & 0 & \cdots & 0 & 0 \\ 0 & 1 & -1 & \cdots & 0 & 0 \\ 0 & 0 & 1 & \cdots & 0 & 0 \\ \vdots & \vdots & \vdots & \cdots & \vdots & \vdots \\ 0 & 0 & 0 & \cdots & 1 & -1 \\ 0 & 0 & 0 & \cdots & 0 & 0 \end{pmatrix} \quad B(v) = \begin{pmatrix} 0 & 0 & 0 & \cdots & 0 & 0 \\ 0 & 0 & 0 & \cdots & 0 & 0 \\ 0 & 0 & 0 & \cdots & 0 & 0 \\ \vdots & \vdots & \vdots & \cdots & \vdots & \vdots \\ 0 & 0 & 0 & \cdots & 0 & 0 \\ 1 & 1 & 1 & \cdots & 1 & 1 \end{pmatrix}.$$

For vertices of degree 1, define 1×1 matrices $A = 1$ and $B = 0$. The matrices A and B referenced above then take a block form:

$$A = \oplus_{v \in V} A(v) \quad \quad \quad = \oplus_{v \in V} B(v)$$

We note that Dirichlet standard boundary conditions are local in the sense of [KPS3] and do not mix derivatives with function values.

We note that Dirichlet standard boundary conditions force continuity across all internal vertices for all elements in the corresponding domain of the self-adjoint extension of Δ^0 . Thus, it is the choice of boundary conditions which ultimately ties the geometry and topology of the quantum graph to the analysis of the corresponding Laplace operator.

We will denote the self-adjoint extension of Δ^0 with Dirichlet standard boundary conditions as Δ . The pair consisting of the metric graph G and the operator Δ is the quantum graph we study.

The spectrum of Δ is discrete and of finite multiplicity. We will denote the spectrum of Δ by $\text{spec}(\Delta)$. We will assume there is at least one boundary vertex and we will list elements of $\text{spec}(\Delta)$ in increasing order with multiplicity:

$$0 < \lambda_1 < \lambda_2 \leq \lambda_3 \leq \dots$$

There is a great deal known about the spectrum for arbitrary self-adjoint boundary conditions. For our purposes it is important that there is a heat kernel which can be written as

$$(2.2) \quad p_G(t, x, y) = \sum_{\lambda \in \text{spec}(\Delta)} e^{-\lambda t} \phi_\lambda(x) \phi_\lambda(y).$$

The heat content of G can then be defined via integration as for domains:

$$(2.3) \quad \begin{aligned} q_G(t) &= \int_G \int_G p_G(t, x, y) dx dy \\ &= \sum_{\lambda \in \text{spec}(\Delta)} e^{-\lambda t} \left(\int_G \phi_\lambda(x) dx \right)^2. \end{aligned}$$

We let $\text{spec}^*(\Delta)$ denote the set of values defined by the Dirichlet standard boundary conditions (ie we disregard multiplicity) for which the corresponding eigenspace is

not orthogonal to constant functions. Then we can write the heat content in a fashion which makes explicit its non-spectral nature:

$$(2.4) \quad q_G(t) = \sum_{\lambda \in \text{spec}^*(\Delta)} a_\lambda^2 e^{-\lambda t}$$

where a_λ^2 is the square of the L^2 -norm of the projection of the constant function 1 on the eigenspace defined by λ .

The moments of $q_G(t)$ define a sequence associated to the quantum graph G . More precisely, as in the introduction, for k a natural number, set

$$A_k = k \int_0^\infty t^{k-1} q_G(t) dt.$$

The moment spectrum of the graph G is the sequence $\{A_k\}_{k=1}^\infty$.

From the definition it is clear that the heat content determines the moment spectrum. The converse (Theorem 1.2 above) is also true:

Theorem 2.2. *The moment spectrum of the quantum graph G determines the heat content of the quantum graph G .*

PROOF The proof follows the case of domains, where the same result holds (see [MM1], [Mc2]). For completeness we provide the argument given in [MM1].

It suffices to show that the moment spectrum determines both $\text{spec}^*(\Delta)$ and the collection of coefficients $\{a_\lambda^2\}$. The important observation is that the moment spectrum describes special values of the Mellin transform of the heat content. More precisely, using (2.4), the Mellin transform of the heat content is given by the Dirichlet series

$$(2.5) \quad \zeta_G(s) = \sum_{\lambda \in \text{spec}^*(\Delta)} a_\lambda^2 \left(\frac{1}{\lambda}\right)^s$$

which converges for real part of s nonnegative and admits a meromorphic extension to the plane, with poles at the negative half-integers (see [MM1]). The moment spectrum then satisfies

$$(2.6) \quad \zeta_G(n) = \frac{A_n}{\Gamma(n+1)}$$

Using (2.5) and (2.6), there is a recursion: Write $\text{spec}^*(\Delta) = \{\mu_n\}_{n=1}^\infty$ with μ_n strictly increasing. Then

$$\mu_1 = \sup \left\{ \mu \geq 0 : \limsup_{n \rightarrow \infty} (\mu)^n \frac{A_n}{\Gamma(n+1)} < \infty \right\}$$

and

$$a_{\mu_1}^2 = \limsup_{n \rightarrow \infty} (\mu_1)^n \frac{A_n}{\Gamma(n+1)}.$$

Having determined μ_j and $a_{\mu_j}^2$ for $j < k$, we have

$$\mu_k = \sup \left\{ \mu \geq 0 : \limsup_{n \rightarrow \infty} (\mu)^n \left(\frac{A_n}{\Gamma(n+1)} - \sum_{j=1}^{k-1} a_{\mu_j}^2 \left(\frac{1}{\mu_j}\right)^n \right) < \infty \right\}$$

and

$$a_{\mu_k}^2 = \limsup_{n \rightarrow \infty} (\mu_k)^n \left(\frac{A_n}{\Gamma(n+1)} - \sum_{j=1}^{k-1} a_{\mu_j}^2 \left(\frac{1}{\mu_j}\right)^n \right).$$

This shows that both $\text{spec}^*(\Delta)$ and the length partition of G are determined by the L^1 -moment spectrum. Using the spectral representation of the heat content (2.3), it is clear that $\text{spec}^*(\Delta)$ and the coefficients a_λ^2 determine the heat content. This proves that the L^1 -moment spectrum determines heat content and completes the proof of Theorem 1.2.

Our primary interest is in A_1 , which, as in the case of smooth domains, can be described via a solution of a Poisson problem on the graph G . More precisely, Let u_1 solve

$$(2.7) \quad \begin{aligned} \Delta u_1 &= -1 \text{ on interior}(G) \\ u_1 &= 0 \text{ on } \partial G. \end{aligned}$$

We can apply Fubini's theorem to interchange the order of integration in the definition of the heat content and $u_1(x)$ to obtain

$$(2.8) \quad A_1 = \int_G u_1(x) dx.$$

Given any quantum graph with Dirichlet standard boundary conditions, the computation of the right-hand-side of (2.8) is an exercise in linear algebra. We compute torsional rigidity for certain pairs of quantum graphs constructed in the next section.

3. THE SUNADA CONSTRUCTION, BCDS PAIRS AND ISOSPECTRAL QUANTUM GRAPHS

As mentioned in the introduction, Buser, Conway, Doyle and Semmler have constructed families of pairs of isospectral planar domains that are not isometric. Their construction and investigation of the resulting pairs is spectacularly simple. To construct families of pairs of isospectral planar domains,

- Fix a seed triangle with edges labeled;
- Reflect the seed about its edges to produce a second generation of labeled triangles;
- For each of the progeny, reflect and label across edges determined by two rules derived from subgroups which are "nearly conjugate" in Sunada's sense
- Iterate
- Interpret the edges as distinct lengths of an acute triangle.

An example of the construction is given in Figure 1: the so-called 7_1 pairs (for complete details see [BCDS]).

Having constructed families of pairs as above, Buser et al prove that the associated pairs are isospectral using the technique of eigenfunction transplantation. Given an eigenfunction f on one domain, say D_1 , they use the process by which the domain is constructed to naturally partition the domain into a collection of isometric subdomains, say $T_{1,i}$ where i indexes the number of triangles occurring in the construction, say $1 \leq i \leq n$. The same procedure carried out on the domain pair, say D_2 , results in a collection $T_{2,i}$, $1 \leq i \leq n$, of isometric subdomains of D_2 . Having partitioned both domains into collections of subdomains, they restrict the given eigenfunction to each subdomain to produce an associated collection of functions, f_i , $1 \leq i \leq n$, on isometric copies of the same subdomain. They then use the geometry of the underlying domains D_1 and D_2 (ie, how the domains are

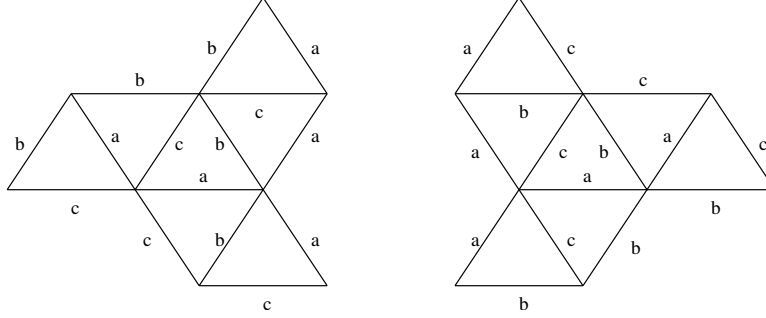


FIGURE 1. Pairs of isospectral non-isometric planar domains

constructed from the collections of subdomains) to construct a linear map which prescribes how to build an associated eigenfunction on the domain D_2 by combining the function elements f_i on each subdomain of D_2 . The process by which an explicit transplantation map is constructed is described neatly in the references [BCDS] and [Ch]. For our purposes it is important to note that the process is essentially combinatorial in the sense that it depends only on the following:

- The eigenfunction f vanishes at the boundary of D_1 .
- To smoothly continue the eigenfunction f across the boundary of the domain D_1 , the reflection principle requires that the value of $f(x^*)$ be prescribed to be $-f(x)$ where x is the reflection image of x^* .
- If T_{1,i_1} and T_{1,i_2} are subdomains which share a boundary internal to D_1 , the associated eigenfunction elements f_{i_1} and f_{i_2} and their respective normal derivatives must match along the common boundary.

There are also techniques to produce *quantum graph* analogs [BPB], [SS], [BSS]. To proceed, we recall the required definitions.

Following earlier work (cf [SS], [BSS], [BPB] and references therein) Band, Parzanchevski and Ben-Shach have described an extension of eigenfunction transplantation in the context of quantum graphs [BPB]. They provide a method which associates to every family of pairs constructed in [BCDS], a family of pairs of quantum graphs which are isospectral but not isometric. The construction technique is straightforward, as is the check that the objects satisfy the required conditions. We sketch the process below and produce the pairs associated to the 7_1 pairs in Figure 2.

For each pair of isospectral nonisometric domains found in [BCDS],

- For each triangle appearing in the BCDS construction, introduce a 3-star graph consisting of three edges, with edges labeled with a label from the edges of the corresponding triangle, joined at a central vertex.
- Join edges in 3-stars at a common degree two vertex if corresponding edges in the triangles to which they are associated overlap.

We carry out the process on quantum graphs corresponding to 7_1 pairs in Figure 3. Note that for the graphs to be isometric, it would be necessary to map the 3-stars corresponding to generating triangles onto each other.

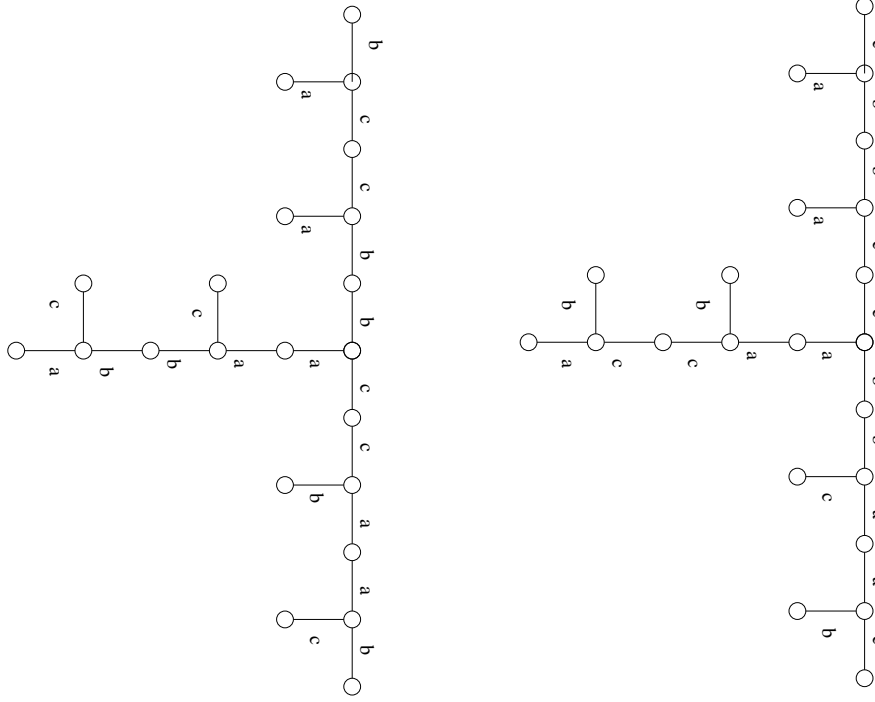


FIGURE 2. Quantum graph analogs of pairs of isospectral non-isometric planar domains

For Neumann standard boundary conditions, the quantum graph analogs are shown to be isospectral and non-isometric in [BSS] (see also [BPB]). This is accomplished by showing that the graphs share the same secular equation. The same argument can be made to work in the current context, but instead we provide an explicit transplantation map. In fact, it's easy to check that the transplantation map used to establish that the BCDS pairs are isometric works to show that the associated quantum graphs pairs are isometric. We do this as follows:

- Label the edges of the quantum graph G_1 and the corresponding partner G_2 .
- Given an eigenfunction on G_1 , restrict to 3-star subgraphs to obtain a collection of functions defined on isometric 3-stars.
- Use the linear map constructed following [BCDS] to construct the required transplantation map taking eigenfunctions of G_1 to eigenfunctions of G_2 .

We can formalize these observations with

Proposition 3.1. *The quantum graph (with Dirichlet standard boundary conditions) analogs of the pairs constructed in [BCDS] are isospectral and non-isometric.*

Proof By construction, for each domain constructed in [BCDS] the corresponding quantum graph is obtained by replacing subdomains with 3-stars, gluing 3-stars along boundaries which correspond to boundaries which are glued in subdomains. The transplantation map for domains may be represented by a matrix acting on function elements defined on subdomains, all of which can be identified. This

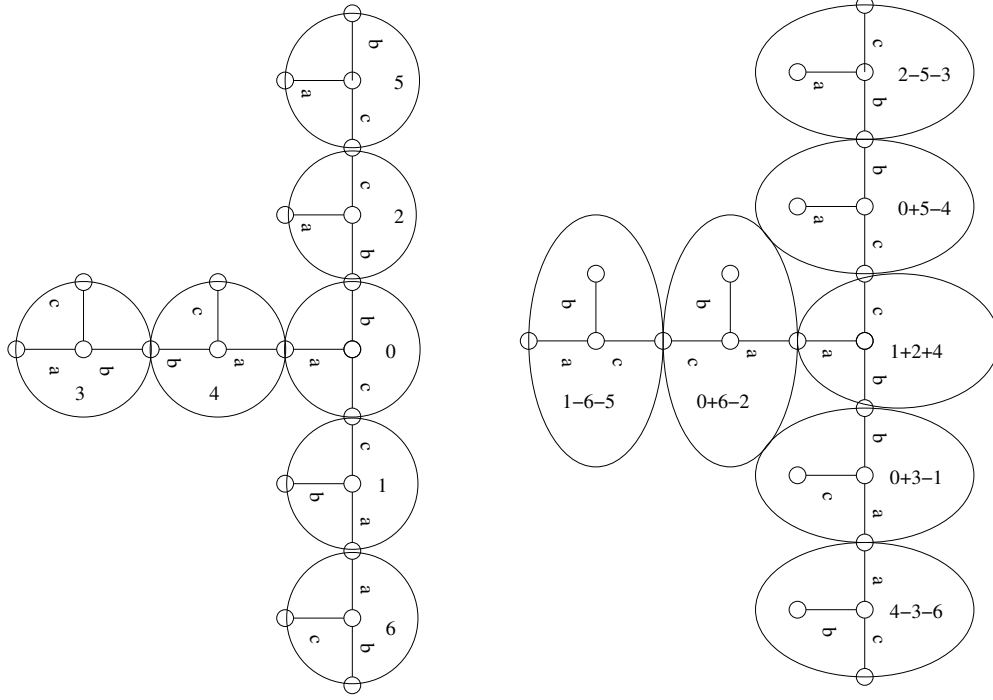


FIGURE 3. Eigenfunction transplantation for quantum graphs

defines a linear map from eigenfunctions on G_1 to functions on G_2 , which we will write as \mathcal{L} . Give an eigenfunction ϕ on G_1 corresponding to eigenvalue λ , to see that the image $\mathcal{L}\phi$ is an eigenfunction on G_2 first note that on the interior of every edge, $\Delta\mathcal{L}\phi = \lambda\mathcal{L}\phi$ by linearity. Thus, it suffices to check that $\mathcal{L}\phi$ has value zero at the boundary of G_2 and that $\mathcal{L}\phi$ behaves as it should across glued edges. But for this to be the case requires only the three properties listed in our description of the transplantation process given above. Since the gluing relations for quantum graphs are precisely those that are prescribed by the domains and the boundary conditions are Dirichlet in both cases, these three properties must hold for the image of ϕ under \mathcal{L} . In particular, $\mathcal{L}\phi$ must be an eigenfunction corresponding to eigenvalue λ .

We give the required transplantation map in Figure 3.

4. COMPUTING TORSIONAL RIGIDITY

We are now in a position to prove Theorem 1.1 for the 7_1 pairs of Figure 2. We begin by noting that we can eliminate vertices of degree 2 and replace the corresponding two edges by a single edge of length equal to the sum of the corresponding edges (following Friedlander [Fr1], we call such quantum graphs *clean*). This results in the pair of quantum graphs given in Figure 4. Note that there is a symmetry: interchanging b and c in the two graphs maps one graph onto the other. We use this symmetry in the computation of the torsional rigidity of each graph.

Suppose we denote by $x_{i,j}$ for the coordinate on the j th edge of the i th graph. Then we must solve

$$\frac{d^2 u_{i,j}}{dx_{i,j}^2} = -1$$

with boundary conditions determined by our choice of Dirichlet standard boundary conditions. The solution on each edge is of the form

$$(4.1) \quad u_{i,j}(x_{i,j}) = -\frac{1}{2}x_{i,j}^2 + \alpha_{i,j}x_{i,j} + \beta_{i,j}$$

where the constants $\alpha_{i,j}$ and $\beta_{i,j}$ are to be determined from the Dirichlet standard boundary conditions. Thus, for each graph there are 30 constants to be determined using nine Dirichlet boundary conditions at vertices of degree 1, seven Kirchoff boundary conditions at vertices of degree 3, and fourteen continuity conditions at vertices of degree 3. This determines a linear system $L\mathbf{a} = \mathbf{v}$ where the coefficient matrix L is a sparse 21×21 matrix and the constant vector \mathbf{v} is defined in terms of continuity constraints and conservation at internal nodes. The structure of the matrix will be determined by our choice of edge labels and orientation. We choose the first nine edges to be those incident to boundary vertices and we orient the edges to be inward facing relative to the boundary. With this choice the coefficients $\beta_{i,j} = 0$ for $i = 1, 2$ and $1 \leq j \leq 9$. With the remaining edges oriented to point toward the "central node", the representation of L for G_1 as pictured in figure 4, is given by the coefficient matrix L_1

$$\begin{pmatrix} c & 0 & 0 & 0 & 0 & 0 & 0 & 0 & 0 & 0 & 0 & 0 & 0 & 0 & 0 & 0 & -1 & 0 & 0 & 0 & 0 & 0 \\ 0 & a & 0 & 0 & 0 & 0 & 0 & 0 & 0 & 0 & 0 & 0 & 0 & 0 & 0 & 0 & -1 & 0 & 0 & 0 & 0 & 0 \\ 0 & 0 & b & 0 & 0 & 0 & 0 & 0 & 0 & 0 & 0 & 0 & 0 & 0 & 0 & 0 & 0 & 0 & 0 & -1 & 0 & 0 \\ 0 & 0 & 0 & a & 0 & 0 & 0 & 0 & 0 & 0 & 0 & 0 & 0 & 0 & 0 & 0 & 0 & 0 & 0 & 0 & -1 & 0 \\ 0 & 0 & 0 & 0 & b & 0 & 0 & 0 & 0 & 0 & 0 & 0 & 0 & 0 & 0 & 0 & 0 & 0 & 0 & 0 & 0 & -1 \\ 0 & 0 & 0 & 0 & 0 & c & 0 & 0 & 0 & 0 & 0 & 0 & 0 & 0 & 0 & 0 & 0 & 0 & 0 & 0 & 0 & -1 \\ 0 & 0 & 0 & 0 & 0 & 0 & a & 0 & 0 & 0 & 0 & 0 & 0 & 0 & 0 & 0 & -1 & 0 & 0 & 0 & 0 & 0 \\ 0 & 0 & 0 & 0 & 0 & 0 & 0 & b & 0 & 0 & 0 & 0 & 0 & 0 & 0 & 0 & 0 & 0 & -1 & 0 & 0 & 0 \\ 0 & 0 & 0 & 0 & 0 & 0 & 0 & 0 & c & 0 & 0 & 0 & 0 & 0 & 0 & 0 & 0 & -1 & 0 & 0 & 0 & 0 \\ 0 & 0 & 0 & 0 & 0 & 0 & 0 & 0 & 0 & 0 & 2b & 0 & 0 & 0 & 0 & 0 & 1 & -1 & 0 & 0 & 0 & 0 \\ 0 & 0 & 0 & 0 & 0 & 0 & 0 & 0 & 0 & 0 & 0 & 2c & 0 & -2a & 0 & 0 & 0 & 1 & 0 & -1 & 0 & 0 \\ 0 & 0 & 0 & 0 & 0 & 0 & 0 & 0 & 0 & 0 & 0 & 0 & -2b & 2a & 0 & 0 & 0 & 0 & -1 & 1 & 0 & 0 \\ 0 & 0 & 0 & 0 & 0 & 0 & 0 & 0 & 0 & 0 & 0 & 0 & 0 & 0 & 2c & 0 & 0 & 0 & 0 & -1 & 1 & 0 \\ 0 & 0 & 0 & 0 & 0 & 0 & 0 & 0 & 0 & 0 & 0 & 0 & 0 & 0 & 0 & 2a & b & 0 & -1 & 0 & 0 & 1 \\ 1 & 1 & 0 & 0 & 0 & 0 & 0 & 0 & 0 & -1 & 0 & 0 & 0 & 0 & 0 & 0 & 0 & 0 & 0 & 0 & 0 & 0 \\ 0 & 0 & 1 & 1 & 0 & 0 & 0 & 0 & 0 & 0 & 0 & 0 & 0 & 0 & -1 & 0 & 0 & 0 & 0 & 0 & 0 & 0 \\ 0 & 0 & 0 & 0 & 1 & 1 & 0 & 0 & 0 & 0 & 0 & 0 & 0 & 0 & 0 & -1 & 0 & 0 & 0 & 0 & 0 & 0 \\ 0 & 0 & 0 & 0 & 0 & 0 & 1 & 0 & 0 & 1 & -1 & 0 & 0 & 0 & 0 & 0 & 0 & 0 & 0 & 0 & 0 & 0 \\ 0 & 0 & 0 & 0 & 0 & 0 & 0 & 1 & 0 & 0 & 0 & -1 & 0 & -1 & 1 & 0 & 0 & 0 & 0 & 0 & 0 & 0 \\ 0 & 0 & 0 & 0 & 0 & 0 & 0 & 0 & 1 & 0 & 0 & -1 & 0 & 0 & 1 & 0 & 0 & 0 & 0 & 0 & 0 & 0 \\ 0 & 0 & 0 & 0 & 0 & 0 & 0 & 0 & 0 & 0 & 1 & 1 & 1 & 0 & 0 & 0 & 0 & 0 & 0 & 0 & 0 & 0 \end{pmatrix}$$

The continuity and conservation constraints define a vector, \mathbf{v}_1 , given by

$$\mathbf{v}_1 = (c^2/2, a^2/2, b^2/2, a^2/2, b^2/2, c^2/2, a^2/2, b^2/2, c^2/2, 2c^2, 2a^2, 2a^2 - 2b^2, 2c^2, 2a^2, a + c, a + b, b + c, a + 2b, b + 2c, 2a + c, 2a + 2b + 2c)^T$$

where "T" denotes transpose. To obtain the data for the second graph, simply interchange b and c .

We can use these systems to carry out the required calculation

$$\begin{aligned} \int_{G_1} u_1(x)dx - \int_{G_2} u_2(x)dx &= \sum_{j=1}^{15} \left[\int_0^{l_{1,j}} u_{1,j}(x_{1,j})dx_{1,j} - \int_0^{l_{2,j}} u_{2,j}(x_{2,j})dx_{2,j} \right] \\ &= \frac{1}{2} \sum_{j=1}^{15} (\alpha_{1,j}l_{1,j}^2 - \alpha_{2,j}l_{2,j}^2) + \sum_{j=1}^{15} (\beta_{1,j}l_{1,j} - \beta_{2,j}l_{2,j}) \\ (4.2) \quad &= \langle L_1^{-1}\mathbf{v}_1, \mathbf{l}_1 \rangle - \langle L_2^{-1}\mathbf{v}_2, \mathbf{l}_2 \rangle \end{aligned}$$

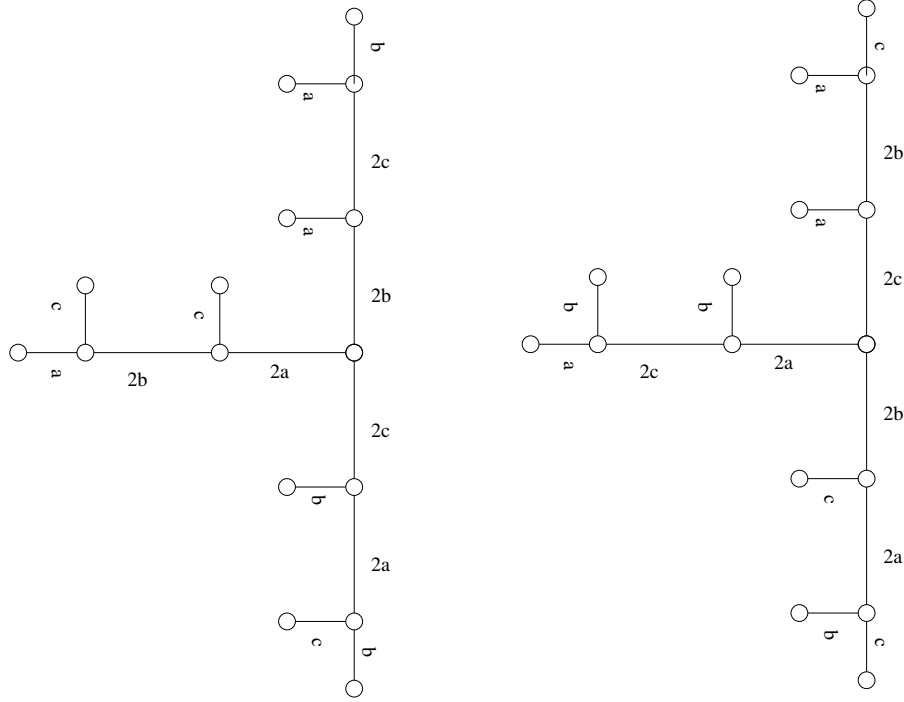


FIGURE 4. Clean pairs of quantum graphs

where the vectors \mathbf{l}_i are constructed from the lengths of the edges of the graphs G_i :

$$\mathbf{l}_1 = 1/2(c^2, a^2, b^2, a^2, b^2, c^2, a^2, b^2, c^2, 4b^2, 4c^2, 4b^2, 4a^2, 4c^2, 4a^2, 4b, 4c, 4b, 4a, 4c, 4a)^T$$

and \mathbf{l}_2 is obtained from \mathbf{l}_1 by interchanging b and c . The right hand side of (4.2) is a rational function in the variables a , b , and c :

$$(4.3) \quad \langle L_1^{-1} \mathbf{v}_1, \mathbf{l}_1 \rangle - \langle L_2^{-1} \mathbf{v}_2, \mathbf{l}_2 \rangle = (a-b)(a-c)(b-c)R(a, b, c)$$

where the rational function $R(a, b, c) = \frac{N(a, b, c)}{D(a, b, c)}$ has a sign:

$$\begin{aligned} N(a, b, c) &= -4(bc + a(b+c))(11a^3(b+c) + bc(11b^2 + 23bc + 11c^2) + \\ &\quad a(b+c)(11b^2 + 48bc + 11c^2) + a^2(23b^2 + 59bc + 23c^2)) \\ D(a, b, c) &= 32a^4(b+c)^2 + 8b^2c^2(4b^2 + 9bc + 4c^2) + 8abc(b+c)(8b^2 + 23bc + 8c^2) + \\ &\quad 8a^3(b+c)(9b^2 + 22bc + 9c^2) + a^2(32b^4 + 248b^3c + 439b^2c^2 + 248bc^3 + 32c^4). \end{aligned}$$

From (4.3) and the explicit expression of $R(a, b, c)$ it is easy to see that the difference in torsional rigidities is nonzero whenever a , b and c are distinct. This proves Theorem 1.1.

As a corollary of Theorem 1.1 and Theorem 1.2, we obtain:

Corollary 4.1. *The quantum graphs G_1 and G_2 are distinguished by their heat content.*

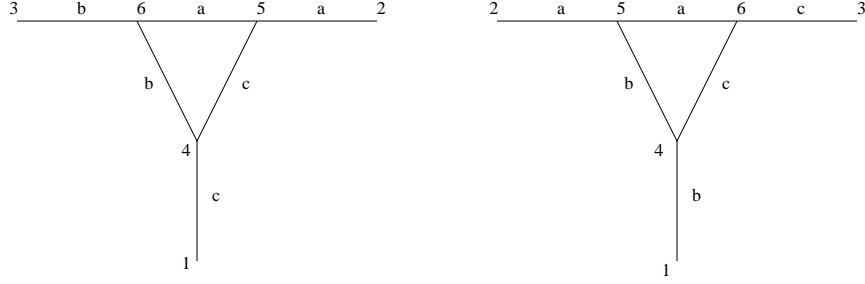


FIGURE 5. Isospectral weighted combinatorial graphs

5. COMBINATORIAL GRAPHS

In [MM2] the authors construct combinatorial weighted graph analogs of BCDS pairs. The result of these constructions for the 7_1 -pairs given above are the two isospectral, non-isomorphic weighted combinatorial graphs given in Figure 5:

There is a natural weighted Laplacian associated to such weighted graphs. For functions on the vertices we write

$$Df(x) = \sum_{y \sim x} W_E(x, y)f(y) - f(x)$$

where the sum is over vertices y adjacent to x and $W_E(x, y)$ denotes the weight along the edge defined by the vertices x and y . For the above two graphs this results in Laplace operators given by

$$D_1 = \begin{pmatrix} a+c & 0 & 0 & -c/2 & 0 & 0 \\ 0 & a+b & 0 & 0 & -a/2 & 0 \\ 0 & 0 & b+c & 0 & 0 & -b/2 \\ -c/2 & 0 & 0 & b+c & -c/2-b/2 & 0 \\ 0 & -a/2 & 0 & -c/2 & a+c & -a/2 \\ 0 & 0 & -b/2 & -b/2 & -a/2 & a+b \end{pmatrix}$$

$$D_2 = \begin{pmatrix} a+b & 0 & 0 & -b/2 & 0 & 0 \\ 0 & a+c & 0 & 0 & -a/2 & 0 \\ 0 & 0 & b+c & 0 & 0 & -c/2 \\ -b/2 & 0 & 0 & b+c & -b/2-c/2 & 0 \\ 0 & -a/2 & 0 & -b/2 & a+b & -a/2 \\ 0 & 0 & -c/2 & -c/2 & -a/2 & a+c \end{pmatrix}$$

It is easy to check that these matrices have the same characteristic equation.

To compute the difference in torsional rigidity for the corresponding combinatorial graphs we let $\mathbf{v} = (1, 1, 1, 1, 1, 1)^T$ and we compute:

$$\langle D_1^{-1} \mathbf{v}, \mathbf{v} \rangle - \langle D_2^{-1} \mathbf{v}, \mathbf{v} \rangle = (a-b)(a-c)(b-c)r(a, b, c)$$

where $r(a, b, c) = \frac{n(a, b, c)}{d(a, b, c)}$ is the rational function defined by

$$n(a, b, c) = 56(bc + a(b+c))$$

$$d(a, b, c) = (32a^4(b+c)^2 + 8b^2c^2(4b^2 + 9bc + 4c^2) + 8abc(b+c)(8b^2 + 23bc + 8c^2) + 8a^3(b+c)(9b^2 + 22bc + 9c^2) + a^2(32b^4 + 248b^3c + 439b^2c^2 + 248bc^3 + 32c^4)).$$

In particular, for distinct values of a , b , and c the isospectral non-isomorphic combinatorial graphs constructed in [MM2] are distinguished by their torsional rigidity.

REFERENCES

- [Br] R. Brooks (1999) *Non Sunada graphs*. Ann. Inst. Four. **49**, 707–725.
- [BSS] R. Band, T. Schapira and U.Smilansky (2006) *Nodal domains on isospectral quantum graphs: the resolution of isospectrality?* J. Phys. A **39** no. 45, 13999–14014
- [BPB] R. Band, O. Parzanchevski and G. Ben-Shach (2009) *The isospectral fruits of representation theory: quantum graphs and drums*. J. Phys. A **42** no. 17, 175202, 42 pp
- [BDK] M. van den Berg, E. Dryden and T. Kappeler (2014) *Isospectrality and heat content*. Bull. London Math. Soc. **46** 793–808.
- [BG] M. van den Berg and P. Gilkey (1994) *Heat content asymptotics for a Riemannian manifold with boundary*. J. Funct. Anal. **120** 48–71.
- [BCDS] P. Buser, J. Conway, P. Doyle and K. Semmler (1994) *Some planar isospectral domains*. Inter. Math. Res. Not. **9** 391–400.
- [GWW] C. Gordon, D. Webb and S. Wolpert (1992) *Isospectral plane domains and surfaces via Riemannian orbifolds*. Invent. Math. **110**, 1–22
- [Gi1] P. Gilkey (2009) *Heat content, heat trace and isospectrality*. New developments in Lie theory and geometry, Contemp. Math., **491** Amer. Math. Soc. Providence, RI 115–123.
- [Fr1] L. Friedlander (2005) *Genericity of simple eigenvalues for a metric graph*. Israel J. Math. **146**, 149–156.
- [KMM] K. J. Kinader, P. McDonald and D. Miller (1998) *Exit time moments, boundary value problems and the geometry of domains in Euclidean space*. Prob. Th. and Rel. **111** 469–487.
- [Mc1] P. McDonald (2002) *Isoperimetric conditions, Poisson problems and diffusions in Riemannian manifolds*. Potential Analysis **16** 115–138.
- [Mc2] P. McDonald (2012) *Exit times, moment problems and comparison theorems*. Potential Analysis **31** 1–8.
- [MM1] P. McDonald and R. Meyers (2003) *Dirichlet spectrum and heat content*. J. Funct. Anal. **200** 150–159.
- [MM2] P. McDonald and R. Meyers (2003) *Isospectral polygons, planar graphs and heat content*. Proc. AMS **131** 3589–3599.
- [KPS1] V. Kostykin, J. Potthoff and R. Schrader (2007) *Heat kernels on metric graphs and a trace formula*. Adventures in mathematical physics, 175–198, Contemp. Math., 447, Amer. Math. Soc., Providence, RI.
- [KPS2] V. Kostykin, J. Potthoff and R. Schrader (2008) *Contraction semigroups on metric graphs*. Analysis on graphs and its applications, 423–458, Proc. Sympos. Pure Math., 77, Amer. Math. Soc., Providence, RI
- [KPS3] V. Kostykin, J. Potthoff and R. Schrader (2005) *Laplacians on metric graphs: eigenvalues resolvents and semigroups* Proceeding of the Conference on Quantum Graphs and Their Applications, Amer. Math. Soc., Providence, RI
- [HMP1] A. Hurtado, S. Markovsen and V. Palmer (2009) *Torsional rigidity of submanifolds with controlled geometry*. Mathem. Ann. **344**, 511–542.
- [HMP2] A. Hurtado, S. Markovsen and V. Palmer (2010) *Comparison of exit moment spectra for extrinsic metric balls*. arXiv 1009.1257v1 [math.DG].
- [BE] J. Bolte and S. Endres (2009) *The trace formula for quantum graphs with general self adjoint boundary conditions*. Ann. Henri Poincaré **10**, 189–223.
- [SS] T. Schapira and U.Smilansky (2006) *Quantum graphs which sound the same in: Non-linear Dynamics and Fundamental Interactions*, F Khanna and D. Matrasulov (eds.), Springer, Berlin 17–29.
- [So] M. Solomyak (2002) *On the eigenvalue estimates for the weighted Laplacian on metric graphs*. Nonlinear problems in mathematical physics and related topics, I, Int. Math. Ser. (N.Y.) vol. 1, Kluwer/Plenum, New York, 327–347.
- [Ch] S. J. Chapman (1995) *Drums that sound the same*. Am. Math. Monthly, 124–138.
- [Po1] G. Plya, *Torsional rigidity, principal frequency, electrostatic capacity and symmetrization*, Quarterly of Applied Math., 6 (1948), pp. 267, 277.

DIVISION OF NATURAL SCIENCE, NEW COLLEGE OF FLORIDA, SARASOTA, FL
E-mail address: `colladay@ncf.edu`

MATHEMATICS DEPARTMENT, Touro COLLEGE, BROOKLYN, NY
E-mail address: `leonkag@gmail.com`

DIVISION OF NATURAL SCIENCE, NEW COLLEGE OF FLORIDA, SARASOTA, FL
E-mail address: `mcdonald@ncf.edu`